

This is a repository copy of *Theoretical rationalisation for the mechanism of N-heterocyclic carbene-halide reductive elimination at Cu-III, Ag-III and Au-III*.

White Rose Research Online URL for this paper:

<https://eprints.whiterose.ac.uk/99758/>

Version: Accepted Version

Article:

Younesi, Yasamin, Nasiri, Bahare, Babaahmadi, Rasool et al. (3 more authors) (2016) Theoretical rationalisation for the mechanism of N-heterocyclic carbene-halide reductive elimination at Cu-III, Ag-III and Au-III. *Chemical Communications*. pp. 5057-5060. ISSN 1364-548X

<https://doi.org/10.1039/c6cc01299j>

Reuse

Other licence.

Takedown

If you consider content in White Rose Research Online to be in breach of UK law, please notify us by emailing eprints@whiterose.ac.uk including the URL of the record and the reason for the withdrawal request.

Theoretical rationalization for the mechanism of *N*-heterocyclic carbene-halide reductive elimination at Cu^{III}, Ag^{III} and Au^{III}

Received 00th January 20xx,
Accepted 00th January 20xx

Yasamin Younesi,^a Bahare Nasiri,^a Rasool BabaAhmadi,^a Charlotte E. Willans,^{*b} Ian J. S. Fairlamb,^{*c} and Alireza Ariafard^{*a,d}

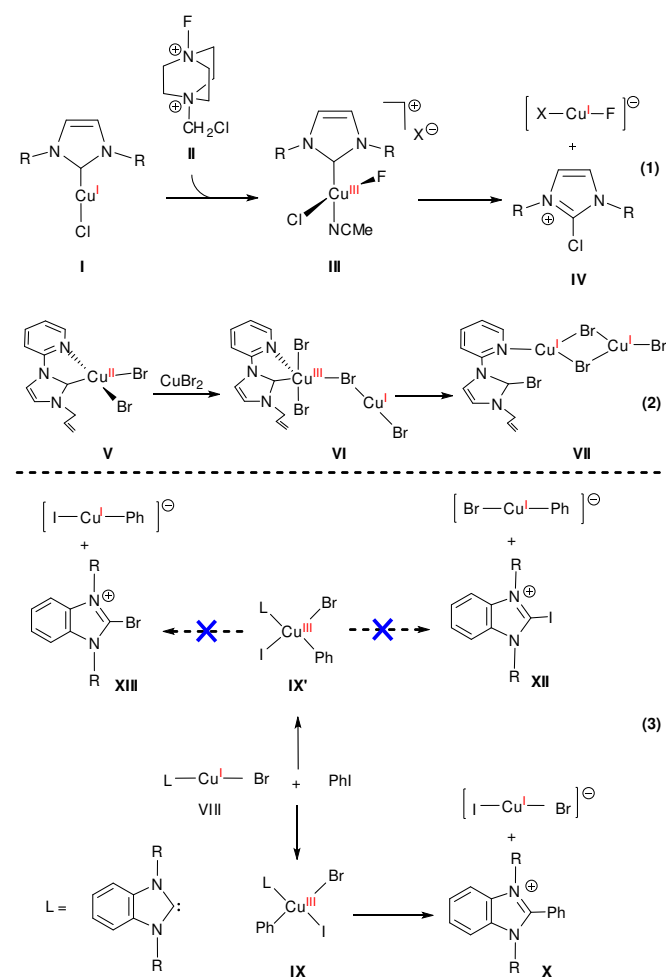
DOI: 10.1039/x0xx00000x

www.rsc.org/

Reductive elimination of imidazolium salts from Cu^{III} is extremely sensitive to the anionic ligand (X or Y) type on Cu (e.g. ΔG^\ddagger ranges from 4.7 kcal/mol to 31.8 kcal/mol, from chloride to benzyl). Weakly σ -donating ligands dramatically accelerate reductive elimination. Comparison with Ag/Au, shows that the HOMO energy, strength of M-NHC and M-Y bonds and inherent stability of M^{III} with respect to M^I are critical to governing reaction feasibility.

N-Heterocyclic carbenes (NHCs) find wide application in organometallic chemistry and catalysis.¹ NHCs serve as spectator ligands and are expected to remain coordinated to the metal centre, playing a stabilising role during, for example, catalysis. Remarkably, NHC ligands can become uncoordinated through key processes like reductive elimination,² migratory insertion³ and ring-opening.^{4,5} The production of 2-haloimidazolium salts from Cu-NHC complexes is a common experimental observation, leading to catalyst decomposition.^{5,6} For example, Stack and co-workers reported that Cu^I complex **I** is oxidized to Cu^{III} intermediate **III** in the presence of the F⁺ oxidant **II** – subsequently 2-haloimidazolium salt **IV** is obtained by reductive elimination from **III** (eq 1).^{6b} Similarly, Willans *et al.* investigated the reaction of **V** with CuBr₂ and found that 2-haloimidazolium salt is generated via reductive elimination preceded by the formation of the Cu^{III} intermediate **VI** (eq 2).^{6c} In contrast, Fairlamb *et al.* observed formation of 2-arylated imidazolium salt **X**, and not 2-haloimidazolium salts **XII** and **XIII**, upon treatment of **VIII** with iodobenzene (eq 3), which is considered a productive reaction pathway in C-H bond activation.⁷ Two transient high oxidation state Cu^{III} intermediates, **IX** and **IX'**, were proposed to form during this reaction. The resultant complex **IX** was found to be reactive toward reductive elimination of 2-arylated imidazolium salt **X**, while intermediate **IX'** is not reactive at all;

the NHC-Y (Y = Br or I) reductive elimination from **IX'** was computed to be extremely endergonic.⁷



^a Department of Chemistry, Faculty of Science, Central Tehran Branch, Islamic Azad University, Shahrak Gharb, Tehran, Iran.

^b School of Chemistry, University of Leeds, Woodhouse Lane, Leeds LS2 9JT, United Kingdom.

^c Department of Chemistry, University of York, Heslington, York YO10 5DD, United Kingdom.

^d School of Physical Science (Chemistry), University of Tasmania, Private Bag 75, Hobart TAS 7001, Australia.

† Electronic Supplementary Information (ESI) available: Computational details, optimized structures, spatial plots of the s-d_z² hybridized orbital, plot of ΔG^\ddagger versus ΔG for NHC-Br elimination from Ag^{III} and Au^{III}, Plot of ΔG versus the s-d_z² hybridized orbital energy of M(Br)(X) (M = Ag, Au), and Cartesian coordinates of all calculated species. See DOI: 10.1039/x0xx00000x

The lack of formation of **XII** and **XIII** (eq 3) provided experimental evidence that the type of anionic ligand likely plays a critical role in the feasibility of imidazolium salt reductive elimination at Cu^{III} . The key aim of the study described herein was to understand how alteration of the anionic ligand at Cu^{III} influences the ease of reductive elimination, where the NHC ligand chemical structure is fixed. To this end, density functional theory (DFT) calculations⁸ have been used to examine the reductive elimination of NHC-Br from *trans*-(NHC) Cu^{III} (Br)₂X complexes, where X = benzyl (Bn), Br, CF₃, CH₃, Cl, I, CN, F, Ph or vinyl, based on the model reaction given in eq 4. The energetics related to the reaction given in eq 4 are listed in Table 1.

The results from the DFT calculations show that NHC-Br reductive elimination from complexes with strongly σ -donating X ligands, such as Ph and CH₃, is energetically unfeasible, while the complexes with weakly σ -donating X ligands, such as Br and Cl, are dramatically reactive in their ability to undergo NHC-Br reductive elimination. As a result of a highly broad range of ΔG^\ddagger from 4.7 to 31.8 kcal/mol and ΔG from -15.5 to 14.6 kcal/mol, the reductive elimination is concluded to be extremely sensitive to the nature of the anionic ligand – a surprising outcome. The higher activation energies for the Cu^{III} complexes with stronger σ -donating X ligands reflect later transition states, *e.g.* **TS^{Cu}_XBr**, an argument which is supported by shorter Br---C(NHC) distances (listed in Table 1).

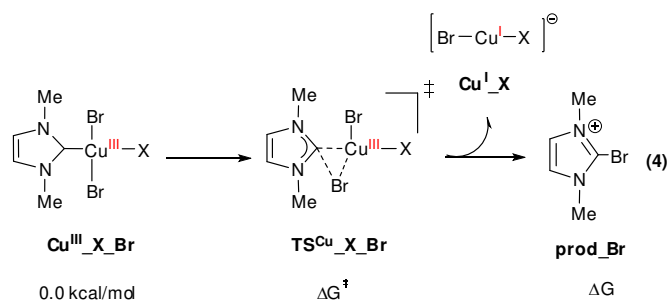


Table 1 Calculated Gibbs activation energy (ΔG^\ddagger), the reaction Gibbs energy (ΔG), the HOMO energy of $\text{Cu}^{\text{I}}\text{X}$ and Br-C(NHC) distance in **TS_XBr** based on the model reductive elimination reaction given in eq 4.

X	ΔG^\ddagger (kcal/mol)	ΔG (kcal/mol)	HOMO energy of $\text{Cu}^{\text{I}}\text{X}$ (eV)	$d_{\text{Br-C(NHC)}}$ in TS^{Cu}_XBr (Å)
Bn	31.8	14.6	-5.08	2.062
CH ₃	30.3	10.3	-5.59	2.037
vinyl	26.6	7.3	-5.77	2.041
Ph	25.1	7.0	-5.82	2.033
CF ₃	15.4	-5.4	-6.38	2.070
CN	10.2	-12.8	-6.87	2.209
I	8.4	-13.8	-6.71	2.312
F	6.5	-6.5	-6.28	2.081
Br	5.7	-15.2	-6.69	2.302
Cl	4.7	-15.5	-6.67	2.312

An excellent linear relationship between ΔG^\ddagger and ΔG with $R^2 = 0.94$ (Fig. 1) suggests that there exists a direct correlation between kinetic and thermodynamic factors of these reactions; the more exergonic the reaction, the lower the activation barrier and conversely the more endergonic the reaction, the higher the activation barrier. The ease of the NHC-Br reductive elimination lies with the intrinsic stability of the resulting Cu^{I} complex $\text{Cu}^{\text{I}}\text{X}$ (*e.g.* 4). The stability of the Cu^{I} complex is directly affected by the identity of the X ligands; the X possessing a strongly σ -donating property makes $\text{Cu}^{\text{I}}\text{X}$ less stable while one with a weak σ -donating property increases stability.

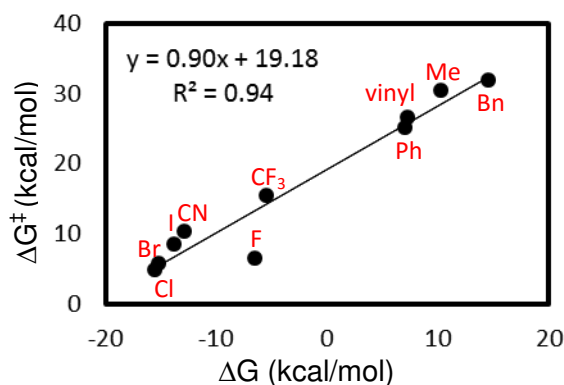


Fig. 1 Plot of ΔG^\ddagger versus ΔG for reductive elimination of NHC-Br from *trans*-(NHC) $\text{Cu}(\text{Br})_2\text{X}$ complexes where X = Bn, CH₃, vinyl, Ph, CF₃, CN, I, F, Br and Cl.

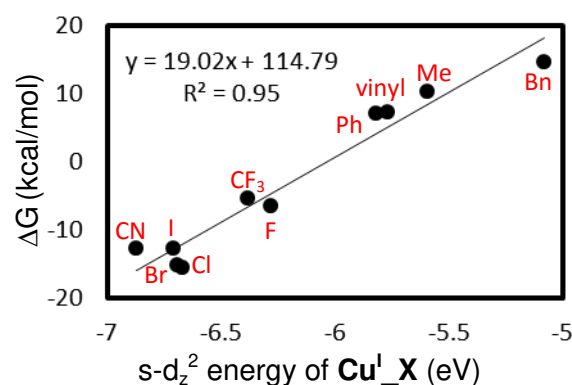


Fig. 2 Plot of ΔG versus the $s\text{-}d_z^2$ hybridized orbital energy of $\text{Cu}(\text{Br})(\text{X})$ ($\text{Cu}^{\text{I}}\text{X}$) complex where X = Bn, CH₃, vinyl, Ph, CF₃, CN, I, F, Br and Cl.

The reason underpinning the stability of Cu^{I} complexes, which is dependent on the nature of X ligand, was probed by molecular orbital analysis of the Cu^{I} complexes as illustrated in Fig. 3. Here the linear ML_2d^{10} complexes with $D_{\infty h}$ geometry, where M is a first-row transition metal, have Σ_g^+ , π_g and Δ_g symmetries for 3d orbital, Σ_g^+ for 4s and Σ_u^+ and Π_u for 4p. On the other hand, symmetry-adapted linear combinations of the in-phase and out-of-phase ligand orbitals have Σ_g^+ and Σ_u^+ symmetries. The Σ_g^+ combination matches with metal 4s and $3d_z^2$ orbitals which give the molecular levels $1\Sigma_g^+$ (bonding), $2\Sigma_g^+$ (slightly anti-bonding) and $3\Sigma_g^+$ (anti-bonding). In this case, $1\Sigma_g^+$ and $3\Sigma_g^+$ are composed of the $s\text{-}d_z^2$ hybridized orbital

while $2\Sigma_g^+$ utilises the $s-d_z^2$ hybridization. The metal p_z orbital interacts with the Σ_u^+ combination and gives two molecular orbitals $1\Sigma_u^+$ and $2\Sigma_u^+$. In such a system, the d_{xz} , d_{yz} , d_{xy} and $d_{x^2-y^2}$ sets remain nonbonding and the $2\Sigma_g^+$ with slightly antibonding character corresponds to the highest occupied molecular orbital (HOMO). The energy of the HOMO is raised as the σ -donating character of the L ligand is increased. Indeed, a stronger σ -donating L ligand gives a greater repulsive interaction with the $s-d_z^2$ hybridized orbital, resulting in an increase in the energy of $2\Sigma_g^+$ orbital and thus a decrease in the stability of Cu^I complex.

It follows that the low stability of the $[\text{Cu}^I(\text{Br})(\text{X})]^-$ complexes, where X = benzyl, methyl, vinyl and phenyl, is related to significant destabilization of their $s-d_z^2$ hybridized orbital. An excellent correlation between the $s-d_z^2$ hybridized orbital energies and the reaction Gibbs free energy (ΔG) with $R^2 = 0.95$ (Fig. 2), confirms the claim showing that Cu^I complex stability is directly affected by the anionic ligand (X) identity.

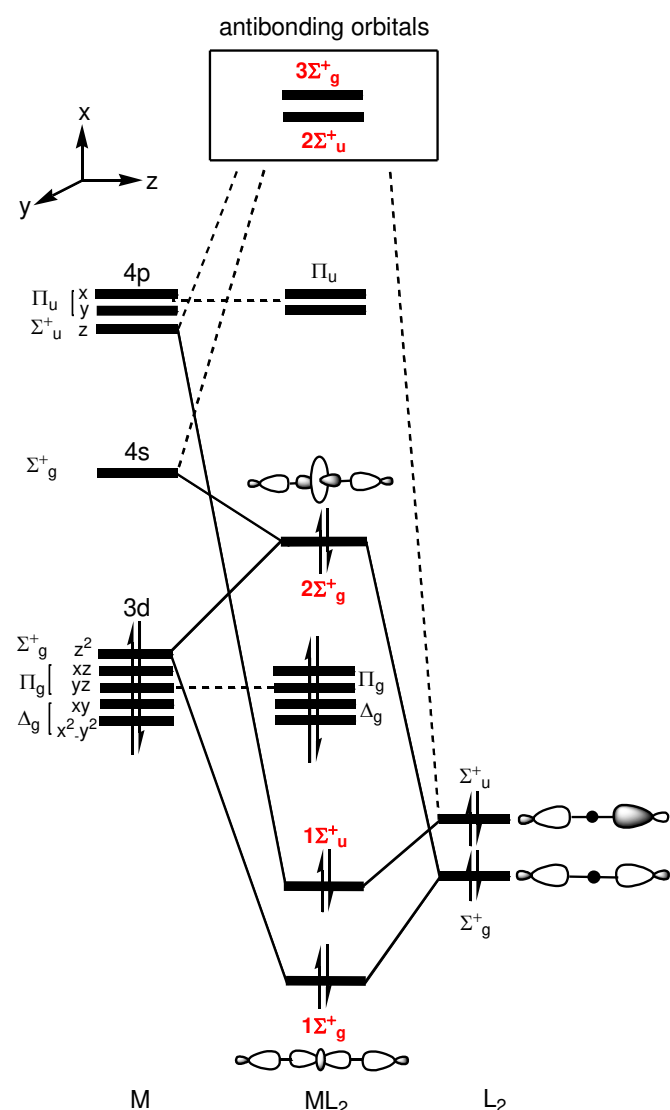


Fig. 3 Schematic molecular orbital diagram for the linear $\text{ML}_2 d^{10}$ complex with $D_{\infty h}$ geometry.

Since a charge separation is involved during the course of NHC-Br reductive elimination, a solvent with a higher dielectric constant (such as acetonitrile, $\epsilon = 37.5$) is expected to facilitate the reaction. Our calculations show that, although in acetonitrile the reaction $\text{Cu}^{\text{III}}\text{-X-Br} \rightarrow \text{Cu}^I\text{-X} + \text{Prod-Br}$ becomes more favourable, the impact of the solvent on the energy of $\text{TS}^{\text{Cu}}\text{-X-Br}$ is not very significant. For example, the reaction free energy and the activation free energy for reaction $\text{Cu}^{\text{III}}\text{-Br-Br} \rightarrow \text{Cu}^I\text{-Br} + \text{Prod-Br}$ in dichloromethane ($\epsilon = 8.93$) are -15.2 and 5.7 kcal/mol respectively, while those in acetonitrile are changed to -21.9 and 5.2 kcal/mol, respectively (for details see Table S3 and Figures S12 and S13).

We next turned our attention to NHC-Br reductive elimination from *trans*-(NHC) $\text{M}(\text{Br})_2\text{X}$ complexes ($\text{M} = \text{Ag}$ and Au) to understand how the nature of metal centre affects the reaction feasibility. Calculations show that reductive elimination from Au complexes is mainly unfavourable while that from Ag complexes is comparable to our estimate for the Cu complexes (Fig. 4). These results explain why the Au^{III} complexes (NHC) $\text{Au}(\text{Br})_2\text{X}$ are experimentally stable, being used as catalysts for organic transformations.⁹ What is noticeable for the (NHC) $\text{M}(\text{Br})_2\text{X}$ complexes of the copper triad is a reasonable correlation between ΔG^\ddagger and ΔG with $R^2 = 0.81$, which means that, regardless of metal centre type, more exergonic reactions tend to give lower activation energies (Fig. 4). In contrast, there is no apparent correlation between the HOMO energy of the $\text{M}^I(\text{Br})(\text{X})$ complexes ($\text{M} = \text{Cu}$, Ag and Au) and ΔG . It is concluded that in addition to the HOMO energy, other factors such as the strength of M-NHC and M-Br bonds as well as inherent stability of M^{III} with respect to M^I can play a crucial role in governing the reaction feasibility.

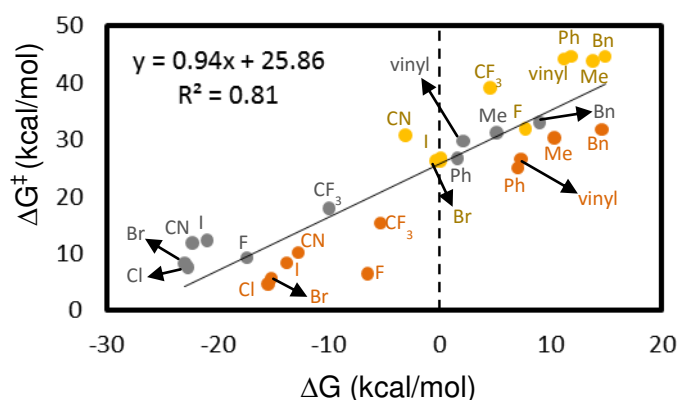


Fig. 4 Plot of ΔG^\ddagger versus ΔG for reductive elimination of NHC-Br from *trans*-(NHC) $\text{M}(\text{Br})_2\text{X}$ complexes, where $\text{M} = \text{Cu}$ (orange points), Ag (grey points) and Au (yellow points).

To rationalise why the Cl ligand in intermediate **III**, instead of F ligand, selectively participates in the reductive elimination (eq 1), the effect of leaving group Y on the ease of the reductive elimination from $\text{Cu}^{\text{III}}\text{-Br-Y}$ was investigated (eq 5). In contrast to the above discussion, a reverse correlation between the reaction energies and the energy barriers was found. Thus, the more exergonic the reaction the higher the activation energy (Table 2). It

follows that the thermodynamic effect does not play a role in controlling the activation energy of the NHC-Y reductive elimination from complexes $\text{Cu}^{\text{III}}\text{-Br}_2\text{-Y}$. The Cu-Y bond strength emerges as a critical factor in the NHC-Y reductive elimination, evidenced by a correlation coefficient (R^2) of 0.98 for homolytic Cu-Y energy in $\text{Cu}^{\text{III}}\text{-Br}_2\text{-Y}$ versus the Gibbs activation energy of the NHC-Y reductive elimination (Fig. 5). Indeed, since $\text{TS}^{\text{Cu}}\text{-Br}_2\text{-Y}$ is intrinsically an early transition state, the $\text{Cu}^{\text{III}}\text{-Y}$ bond strength is much more important than the ΔG thermodynamic effect in governing the reductive elimination barrier.

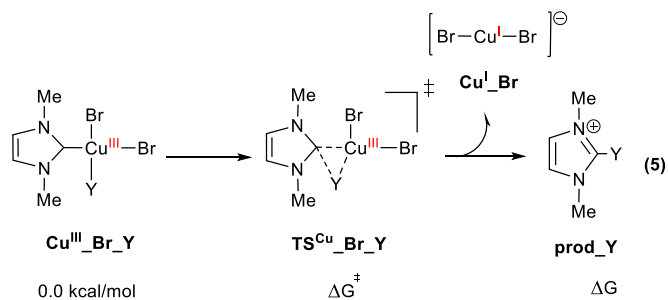


Table 2 Calculated Gibbs activation energy (ΔG^\ddagger), the reaction Gibbs energy (ΔG) and the Cu-Y bond dissociation energy in $\text{Cu}^{\text{III}}\text{-Br}_2\text{-Y}$ [$D_e(\text{Cu-Y})$] for the model reductive elimination reaction given in eq 5.

Y	ΔG^\ddagger (kcal/mol)	ΔG (kcal/mol)	$D_e(\text{Cu-Y})$ in $\text{Cu}^{\text{III}}\text{-Br}_2\text{-Y}$ (kcal/mol)
F	12.4	-32.7	59.4
Cl	8.5	-18.1	43.3
Br	5.7	-15.2	31.4
I	2.3	-13.3	24.3

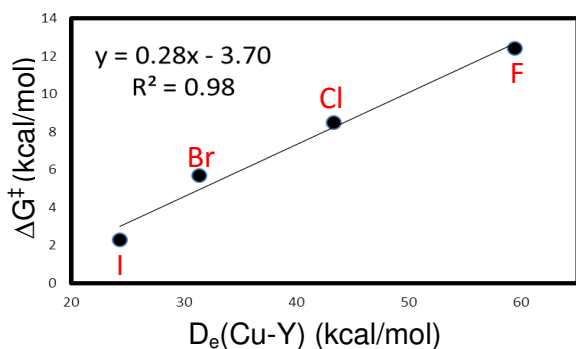


Fig. 5 Plot of the Cu-Y bond strength in $\text{Cu}^{\text{III}}\text{-Br}_2\text{-Y}$ [$D_e(\text{Cu-Y})$] versus ΔG^\ddagger where Y = F, Cl, Br and I.

In conclusion, the activation barrier for imidazolium salt reductive elimination from a Cu^{III} complex is dependent on the inherent stability of the resultant Cu^{I} complex, whereas for a given anionic ligand, it is principally controlled by bond strength of the $\text{Cu}^{\text{III}}\text{-leaving group}$. The stability of Cu^{I} complexes is reliant on the extent of repulsion experienced by their $s\text{-}d_z^2$ hybridized orbital; the strong σ -donating ligands decreases the stability of Cu^{I} complexes. Conversely, the Cu^{I} complexes, with a more destabilized $s\text{-}d_z^2$ hybridized orbital are more prone to undergoing oxidative addition reactions. By studying related Ag and Au complexes we have

determined that the HOMO energy of the resultant M^{I} complex, strength of $\text{M}^{\text{III}}\text{-NHC}$ and $\text{M}^{\text{III}}\text{-Br}$ bonds and inherent stability of M^{III} with respect to M^{I} are critical to governing reaction feasibility.

Notes and references

- The dichotomous reactivity of both carbenes and carbenoids can be finely tuned according to stereoelectronic effects, which is of direct relevance to our work; see: (a) In Contemporary Carbene Chemistry, R. A. Moss, M. P. Doyle Eds., Wiley-VCH, ISBN: 978-1-118-23795-3, 2014. Also, see: (b) N-Heterocyclic Carbenes: Effective Tools for Organometallic Synthesis, S. P. Nolan (Ed.), Wiley-VCH, ISBN: 978-3-527-33490-2, 2014. (c) N-Heterocyclic Carbenes in Transition Metal Catalysis and Organocatalysis, C. Cazin (Ed.), Springer Science, ISBN: 978-90-481-2865-5, 2011.
- (a) D. Bacciu, K. J. Cavell, I. A. Fallis, L. L. Ooi, *Angew. Chem., Int. Ed.*, 2005, **44**, 5282–5284; (b) D. J. Nielsen, A. M. Magill, B. F. Yates, K. J. Cavell, B. W. Skelton, A. H. White, *Chem. Commun.*, 2002, 2500–2501.
- (a) E. Becker, V. Stingl, G. Dazinger, M. Puchberger, K. Mereiter, K. Kirchner, *J. Am. Chem. Soc.*, 2006, **128**, 6572–6573; (b) A. A. Danopoulos, N. Tsoureas, J. C. Green, M. B. Hursthouse, *Chem. Commun.*, 2003, 756–757; (c) S. Fantasia, H. Jacobsen, L. Cavallo, S. P. Nolan, *Organometallics*, 2007, **26**, 3286–3288.
- (a) A. W. Waltman, T. Ritter, R. H. Grubbs, *Organometallics*, 2006, **25**, 4238–4239; (b) C. Segarra, E. Mas-Marza, M. Benitez, J. A. Mata, E. Peris, *Angew. Chem., Int. Ed.*, 2012, **51**, 10841–10845.
- For a review, see: C. E. Willans, B. R. M. Lake, and M. R. Chapman, *Organomet. Chem.*, 2015, **40**, 107–139 (ISBN: 978-1-84973-984-9). For a review beyond catalysis, see: L. Mercks and M. Albrecht, *Chem. Soc. Rev.*, 2010, **39**, 1903–1912.
- (a) E. L. Kolychev, V. V. Shuntikov, V. N. Khrustalev, A. A. Busha, M. S. Nechaev, *Dalton Trans.*, 2011, **40**, 3074–3076; (b) B. L. Lin, P. Kang, T. D. P. Stack, *Organometallics*, 2010, **29**, 3683–3685; (c) B. R. M. Lake, A. Ariafard, C. E. Willans, *Chem. Eur. J.*, 2014, **20**, 12729–12733.
- T. J. Williams, J. T. W. Bray, B. R. M. Lake, C. E. Willans, Nasir A. Rajabi, A. Ariafard, C. Manzini, F. Bellina, A. C. Whitwood, I. J. S. Fairlamb, *Organometallics*, 2015, **34**, 3497–3507.
- The geometry optimizations were carried out at the B3LYP/LANL2DZ-6-31G(d) level and the single-point calculations were carried out at the M06/def2-QZVP-6-311+G(2d,p) level. For all the calculations the continuum CH_2Cl_2 solvent effects using the CPCM approach were considered (for details see the ESI).
- (a) J. P. Reeds, M. P. Healy, and I. J. S. Fairlamb, *Catal. Sci. Technol.*, 2014, **4**, 3524–3533. (b) J. P. Reeds, A. C. Whitwood, M. P. Healy, and I. J. S. Fairlamb, *Organometallics*, 2013, **32**, 3108–3120. (c) J. P. Reeds, A. C. Whitwood, M. P. Healy, and I. J. S. Fairlamb, *Chem. Commun.*, 2010, **46**, 2046–2049. For recent reviews on Au^{III} complexes and Au catalysis in general, see: (d) A. S. K. Hashmi, *Angew. Chem. Int. Ed.*, 2012, **51**, 12935–12936. (e) C. M. Friend, and A. S. K. Hashmi, *Acc. Chem. Res.*, 2014, **47**, 729–730. For an interesting recent paper involving Au^{III} complexes containing cyclic (alkyl)(amino)carbenes, see: (f) A. S. Romanov, and M. Bochmann, *Organometallics*, 2015, **34**, 2439–2454.